Anomalous $WW\gamma$ vertex in γp collisions

S. Atağ* and İ. T. Çakır
Department of Physics, Faculty of Sciences, Ankara University, 06100 Tandogan, Ankara, Turkey
(Received 9 June 2000; published 9 January 2001)

The potential of a LC+DESY HERAp based γp collider to probe the $WW\gamma$ vertex is presented through a discussion of the sensitivity to anomalous couplings and p_T distribution of the final quark. The limits obtained for $\Delta\kappa$ are comparable to the one which is expected from CERN LHC. The bounds on the anomalous couplings are also found from a corresponding ep collider using the Weizsäcker-Williams approximation to compare with real photons.

DOI: 10.1103/PhysRevD.63.033004 PACS number(s): 14.80.Bn, 12.60.−i, 13.85.Rm

I. INTRODUCTION

Recently there have been intensive studies to test the deviations from the standard model (SM) at present and future colliders. The investigation of three gauge boson couplings plays an important role to manifest the non-Abelian gauge symmetry in standard electroweak theory. The precision measurement of the triple vector boson vertices will be the crucial test of the structure of the SM.

Measurements at the Fermilab Tevatron and CERN e^+e^- collider LEP2 provide present collider limits on anomalous couplings. Recent results from D0 for $WW\gamma$ couplings are given by $-0.25<\Delta\kappa<0.39$ ($\lambda=0$) and $-0.18<\lambda<0.19$ ($\Delta\kappa=0$) at 95% C.L., assuming the $WW\gamma$ couplings are equal to the WWZ couplings [1]. Individual experiments by the ALEPH, DELPHI, L3, and OPAL Collaborations at LEP2 give the same order of sensitivity as the Tevatron [2]. As an example, DELPHI has the 95% C.L. limits of $-0.46<\Delta\kappa<0.84$ and $-0.44<\lambda<0.24$. A combination of the measurements of triple gauge boson couplings from the four LEP2 experiments improves the precision to $-0.09<\Delta\kappa<0.15$ ($\lambda=0$) and $-0.066<\lambda<0.035$ ($\Delta\kappa=0$) where the WWZ coupling is kept at the SM value for both cases [3]. Analyses of the $WW\gamma$ vertex has been given by several papers for the DESY ep collider HERA [4–9]. The CERN Large Hadron Collider (LHC) is expected to place better limits on these couplings of $O(10^{-2})$ for $\Delta\kappa$ and $O(10^{-3})$ for λ [10]. Linear electron-positron colliders (LC) will improve further upon the LHC precision by one order of magnitude [11].

After LC is constructed γe, $\gamma\gamma$, linac-ring type ep and γp modes should be discussed and may work as complementary to basic colliders. The Linear Collider design at DESY [11,12] is the only one that can be converted into an ep [13,14] collider. γp collider mode is an additional advantage of this linac-ring-type ep collider [15,16] where real gamma beam is obtained by the Compton backscattering of laser photons off linear electron beam. Estimations show that the luminosity for γp collision turns out to be of the same order as the one for ep collision due to the fact that $\sigma_p \gg \sigma_\gamma$ where σ_p and σ_γ are transverse sizes of proton and photon bunches at collision point. Since most of the photons are produced at the high-energy region in the Compton backscattering the cross sections are about one order of magnitude larger than parental ep collider for photoproduction processes. According to present project at DESY linear electron beam is designed to provide 300, 500, and 800 GeV energy. In the ep collider mode the linac e beam is allowed to collide 920 GeV protons from the HERA ring [13,14]. Parameters of this LC+HERAp and its γp option are shown in Table I [15]. Therefore such, high-energy γp colliders will possibly give additional information to linac-ring type ep colliders for a variety of processes [16,17]. In this paper we examine the potential of future LC+HERAp based γp collider to probe anomalous $WW\gamma$ coupling and compare the results with those from its basic ep collider and other projected future colliders.

II. LAGRANGIAN AND CROSS SECTIONS

C and P parity conserving effective Lagrangian for two charged W boson and one photon interaction can be written following the papers [18,19]:

$$\frac{iL}{g_{WW\gamma}} = g_1^\gamma (W^\dagger_{\mu\nu} W^\mu A^\nu - W^{\mu\nu} W^\dagger_\mu A_\nu) + \kappa W^\dagger_\mu W_\nu A^{\mu\nu} + \frac{\lambda}{M_W^2} W^\dagger_{\rho\mu} W^\mu_\nu A^{\nu\rho}, \tag{1}$$

where

$$g_{WW\gamma}=e, \quad g_1^\gamma=1, \quad W_{\mu\nu}=\partial_\mu W_\nu - \partial_\nu W_\mu$$

and dimensionless parameters κ and λ are related to the magnetic dipol and electric quadrupole moments. For $\kappa=1$

TABLE I. Main parameters of LC+HERAp based ep and γp colliders.

LC	HERAp	$\sqrt{s_{ep}}$ (GeV)	$\sqrt{s_{\gamma p}}^{\max}$ (GeV)	$L_{ep} \simeq L_{\gamma p}$ (cm^{-1} s^{-1})
300	920	1050.7	957.2	1×10^{31}
500	920	1356.5	1235.8	1×10^{31}
800	920	1715.8	1563.2	1×10^{31}

*Corresponding author. Email address: atag@science.ankara.edu.tr

and $\lambda=0$ standard model is restored. In momentum space this has the following form with momenta $W^+(p_1), W^-(p_2)$ and $A(p_3)$:

$$\begin{aligned}\Gamma_{\mu\nu\rho}(p_1,p_2,p_3)\\ =e\bigg[&g_{\mu\nu}\left(p_1-p_2-\frac{\lambda}{M_W^2}[(p_2\cdot p_3)p_1-(p_1\cdot p_3)p_2]\right)_\rho\\ &+g_{\mu\rho}\left(\kappa p_3-p_1+\frac{\lambda}{M_W^2}[(p_2\cdot p_3)p_1-(p_1\cdot p_2)p_3]\right)_\nu\\ &+g_{\nu\rho}\left(p_2-\kappa p_3-\frac{\lambda}{M_W^2}[(p_1\cdot p_3)p_2-(p_1\cdot p_2)p_3]\right)_\mu\\ &+\frac{\lambda}{M_W^2}(p_{2\mu}p_{3\nu}p_{1\rho}-p_{3\mu}p_{1\nu}p_{2\rho})\bigg], \end{aligned} \tag{2}$$

where $p_1+p_2+p_3=0$. There are three Feynman diagrams for the subprocess $\gamma q_i\to W q_j$ and only t-channel W exchange graph contributes $WW\gamma$ vertex. One should note that γp collision isolates $WW\gamma$ coupling but many processes in e^+e^-, pp, and ep collisions include mixtures of $WW\gamma$ and WWZ couplings.

The unpolarized differential cross section for the subprocess $\gamma q_i\to W q_j$ can be obtained using helicity amplitudes from [7] summing over the helicities

$$\frac{d\hat{\sigma}}{d\hat{t}}=\frac{2}{\hat{s}-M_W^2}\frac{\beta}{64\pi\hat{s}}\sum_{\lambda_\gamma\lambda_W}\frac{1}{2}M^2_{\lambda_\gamma\lambda_W}, \tag{3}$$

where

$$M_{\lambda_\gamma\lambda_W}=\frac{e^2}{\sqrt{2}\sin\theta_W}\frac{\hat{s}}{\hat{s}+M_W^2}\sqrt{\beta}A_{\lambda_\gamma\lambda_W},\quad \beta=1-\frac{M_W^2}{\hat{s}} \tag{4}$$

and θ_W is the Weinberg angle.

For the signal we are considering a quark jet and on-shell W with leptonic decay mode

$$\gamma p\to W^{\mp}+\text{jet}\to l+p_T^{\text{miss}}+\text{jet},\quad l=e,\mu. \tag{5}$$

In this mode charged lepton and the quark jet are in general well separated and the signal is in principle free of background of SM.

The total cross section for the subprocess $\gamma q_i\to W q_j$ can be divided into two parts, direct, and resolved-photon production

$$\hat{\sigma}=\hat{\sigma}_{\text{dir}}+\hat{\sigma}_{\text{res}}. \tag{6}$$

The direct part is given as follows

$$\begin{aligned}\hat{\sigma}=&\frac{\alpha G_F M_W^2}{\sqrt{2}\hat{s}}|V_{q_iq_j}|^2\Bigg\{(|e_q|-1)^2(1-2\hat{z}+2\hat{z}^2)\log\left(\frac{\hat{s}-M_W^2}{\Lambda^2}\right)-\bigg[(1-2\hat{z}+2\hat{z}^2)-2|e_q|(1+\kappa+2\hat{z}^2)\\ &+\frac{(1-\kappa)^2}{4\hat{z}}-\frac{(1+\kappa)^2}{4}\bigg]\log\hat{z}+\left[\left(2\kappa+\frac{(1-\kappa)^2}{16}\right)\frac{1}{\hat{z}}+\left(\frac{1}{2}+\frac{3(1+|e_q|^2)}{2}\right)\hat{z}+(1+\kappa)|e_q|-\frac{(1-\kappa)^2}{16}+\frac{|e_q|^2}{2}\right](1-\hat{z})\\ &-\frac{\lambda^2}{4\hat{z}^2}(\hat{z}^2-2\hat{z}\log\hat{z}-1)+\frac{\lambda}{16z}(2\kappa+\lambda-2)[(\hat{z}-1)(\hat{z}-9)+4(\hat{z}+1)\log\hat{z}]\Bigg\}, \end{aligned} \tag{7}$$

where $\hat{z}=M_W^2/\hat{s}$ and Λ^2 is cut off scale in order to regularize $\hat{u}$ pole of the colinear singularity for massles quarks. In the case of massive quarks there is no need such a kind of cut. The resolved-photon production cross section can be calculated using Breit-Wigner formula for $q_\gamma q_p\to W$ fusion process

$$\hat{\sigma}(q_i\overline{q_j}\to W)=\frac{\pi\sqrt{2}}{3}G_F m_W^2|V_{ij}|^2\delta(x_ix_js_{\gamma p}-m_W^2), \tag{8}$$

where V_{ij} is the Cabibbo-Kobayashi-Maskawa (CKM) matrix. For the integrated cross sections we need parton distribution functions inside the photon and proton. The photon structure function $f_{q/\gamma}$ consists of perturbative pointlike parts and hadronlike parts. The pointlike part can be calculated in the leading logarithmic approximation and is given by the expression

$$f^{LO}_{q/\gamma}(x,Q^2_\gamma)=\frac{3\alpha e_q^2}{2\pi}[x^2+(1-x)^2]\log\frac{Q^2_\gamma}{\Lambda^2}, \tag{9}$$

where e_q is the quark charge. For the integrated total cross section over the quark distributions inside the proton, photon, and the spectrum of backscattered laser photon the following result can be obtained easily:

$$\begin{aligned}\sigma_{\text{res}}=\sigma_0\int_{m_W^2/s}^{0.83}dx\int_x^{0.83}\frac{dy}{xy}f_{\gamma/e}(y)f_{q_i/p}\left(\frac{m_W^2}{xs},Q_p\right)\\ \times\left[f_{q_j/\gamma}\left(\frac{x}{y},Q^2_\gamma\right)-f^{LO}_{q_j/\gamma}\left(\frac{x}{y},Q^2_\gamma\right)\right]\end{aligned} \tag{10}$$

TABLE II. Integrated total cross section times branching ratios $\sigma(\gamma p\rightarrow Wj)\times B(W^+\rightarrow\mu\nu)$ in pb to indicate direct and resolved photon contribution depending on invariant kinematical cut Λ in GeV. DG and MRS A were used for photon and proton structure functions. $\sqrt{s}=1715.8$ GeV.

κ, λ	$\sigma_{\rm dir}\times B(W^+\rightarrow\mu\nu)$ $\Lambda=0.2$	$\Lambda=1$	$\Lambda=5$
1,0	15.79	14.88	13.98
1,1	39.57	38.66	37.75
1,2	110.89	109.98	109.07
0,0	10.48	9.57	8.66
2,0	29.03	28.12	27.21
	$\sigma_{\rm res}\times B(W^+\rightarrow\mu\nu)$		
	-0.62	1.62	3.85

with

$$\sigma_0=\frac{\pi\sqrt{2}}{3s}G_F m_W^2|V_{ij}|^2. \tag{11}$$

Since the contribution from the pointlike part of the photon structure function was already taken into account in the calculation of the direct part it was subtracted from $f_{q/\gamma}(x,Q_\gamma^2)$ in the above formula to avoid double counting on the leading logarithmic level. In a similar way direct part of the integrated cross section can be obtained

$$\sigma_{\rm dir}=\int_{\tau_{\rm min}}^{0.83}d\tau\int_{\tau/0.83}^{1}\frac{dx}{x}f_{\gamma/e}(\tau/x)f_{q/p}(x,Q^2)\hat{\sigma}(\tau s) \tag{12}$$

with $\tau_{\rm min}=(M_W+M_q)^2/s$.

The sum of resolved and direct contribution, in principle, should not depend on value of the parameter Λ. The effects of Λ on the cross sections and contributions of direct and resolved parts are given in Table II. In Table III integrated total cross sections times branching ratio of $W\rightarrow\mu\nu$ and corresponding number of events are shown for various values of κ and λ. Through the calculations proton structure functions of Martin, Robert, and Stirling (MRS A) [20] and photon structure functions of Drees and Grassie (DG) [21] have been used with $Q^2=M_W^2$. Here number of events has been calculated using

$$N=\sigma(\gamma p\rightarrow W+\text{jet})B(W\rightarrow\mu\nu)AL_{\rm int}, \tag{13}$$

where we take the acceptance in the muon channel A and integrated luminosity $L_{\rm int}$ as 65% and 200 pb^{-1}. To give an idea about the comparison with corresponding *ep* collider the cross sections obtained using Weizsäcker-Williams approximation are also shown on the same table. As the cross section $\sigma(\gamma p\rightarrow W+\text{jet})$ we have considered the sum of $\sigma(\gamma u\rightarrow W^+d)$, $\sigma(\gamma\bar{d}\rightarrow W^+\bar{u})$, $\sigma(\gamma\bar{s}\rightarrow W^+\bar{c})$, $\sigma(\gamma u\rightarrow W^+s)$, $\sigma(\gamma\bar{s}\rightarrow W^+\bar{u})$, and $\sigma(\gamma\bar{d}\rightarrow W^+\bar{c})$. As shown from Table III the cross sections using backscattered laser photons are considerably larger than the case of corresponding *ep* collision. We assume that the form factor structure of $\kappa-1$ and λ do not depend on the momentum transfers at the energy region considered. Then anomalous terms containing κ grow with $\sqrt{\hat{s}}/M_W$ and terms with λ rise with $\hat{s}/M_W^2$. Deviation $\Delta\kappa=\kappa-1=1$ from SM value changes the total cross sections 30–70 % whereas the $\Delta\lambda=\lambda=1$ gives 80% changes. Therefore high energy will improve the sensitivity to anomalous couplings. For comparison with HERA energy $\sqrt{s}=314$ GeV the similar results would be 20–40 % for $\Delta\kappa=1$ and 5% for $\Delta\lambda=1$.

TABLE III. Integrated total cross section times branching ratio $\sigma(\gamma p\rightarrow Wj)\times B(W^+\rightarrow\mu\nu)$ in pb and corresponding number of events (in parentheses) without cutoff for massive quarks. $\sqrt{s}=1715.8$ GeV and integrated luminosity $L_{\rm int}=200$ pb^{-1} have been used.

Back scattered laser	*WWA*	κ	λ
17.7(2297)	2.2(288)	1	0
41.4(5388)	3.9(504)	1	1
112.8(14660)	8.9(1151)	1	2
12.4(1606)	1.6(206)	0	0
30.9(4018)	3.7(477)	2	0

It is important to see how the anomalous couplings change the shape of the transverse momentum distributions of the final quark jet. For this reason we use the following formula:

$$\frac{d\sigma}{dp_T}=2p_T\int_{y^-}^{y^+}dy\int_{x_a^{\rm min}}^{0.83}dx_a f_{\gamma/e}(x_a)f_{q/p}(x_b,Q^2)\times\left(\frac{x_a x_b s}{x_a s-2m_T E_p e^y}\right)\frac{d\hat{\sigma}}{d\hat{t}}, \tag{14}$$

where

$$y^{\mp}=\log\left[\frac{0.83s+m_q^2-M_W^2}{4m_T E_p}\mp\left\{\left(\frac{0.83s+m_q^2-M_W^2}{4m_T E_p}\right)^2-\frac{0.83E_e}{E_p}\right\}^{1/2}\right], \tag{15}$$

$$x_a^{(1)}=\frac{2m_T E_p e^y-m_q^2+M_W^2}{s-2m_T E_e e^{-y}},\quad x_a^{(2)}=\frac{(M_W+m_q)^2}{s},$$

$$x_a^{\rm min}=\max(x_a^{(1)},x_a^{(2)}),\quad x_b=\frac{2m_T E_e x_a e^{-y}-m_q^2+M_W^2}{x_a s-2m_T E_p e^y} \tag{16}$$

with

$$\hat{s}=x_a x_b,\quad \hat{t}=m_q^2-2E_e x_a m_T e^{-y},\quad \hat{u}=m_q^2+M_W^2-\hat{s}-\hat{t}$$

$$m_T^2=m_q^2+p_T^2. \tag{17}$$

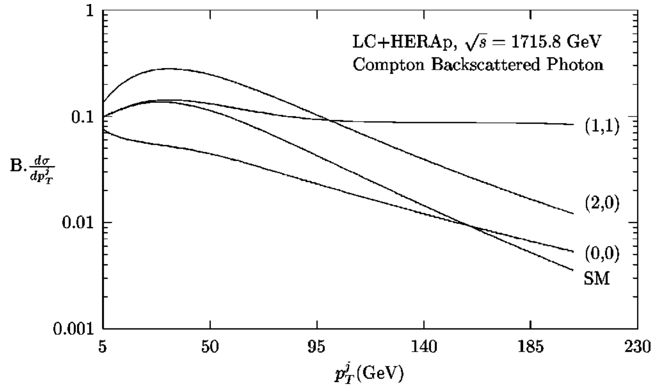

FIG. 1. κ and λ dependence of the transverse momentum distribution of the quark jet at LC+HERA*p* based γp collider (Compton back scattered photon). The unit of the vertical axis is pb/GeV and the numbers in the parentheses stand for anomalous coupling parameters (κ,λ).

The p_T spectrum $B(W\rightarrow\mu\nu)\times d\sigma/dp_T$ of the quark jet is shown in Fig. 1 for various κ and λ values at LC+HERA*p* based γp collider. Similar distribution is given in Fig. 2 for the Weizsäcker-Williams approximation that covers the major contribution from ep collision. It is clear that the cross section at large p_T is quite sensitive to anomalous $WW\gamma$ couplings. As λ increases the cross section grows more rapidly when compared with κ dependence at high p_T region $p_T > 100$ GeV. The cross sections with real gamma beam are one order of magnitude larger than the case of *WWA*. Comparison between two figures also shows that the curves become more separable as $\hat{s}$ gets large.

III. SENSITIVITY TO ANOMALOUS COUPLINGS

We can estimate sensitivity of LC+HERA*p* based γp collider to anomalous couplings by assuming the 0.05 combined systematic error in the luminosity measurement and detector acceptance for the integrated luminosity values of 200 and 500 pb^{-1}. We use the simple χ^2 criterion to obtain sensitivity:

$$\chi^2=\sum_{i=\text{bins}}\left(\frac{X_i-Y_i}{\Delta_i^{\text{exp}}}\right)^2, \tag{18}$$

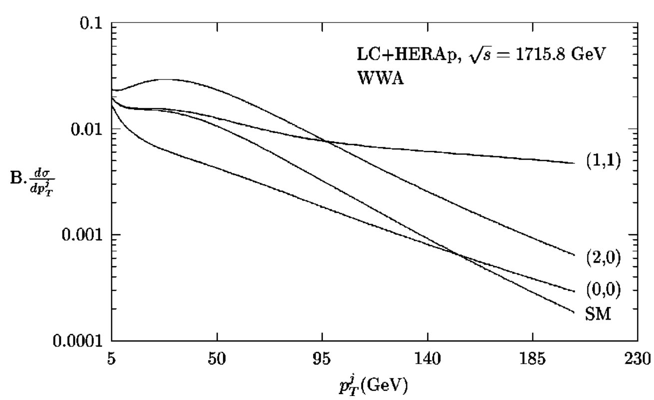

FIG. 2. The same as the Fig. 1 but for the Weizsäcker-Williams approximation.

TABLE IV. Sensitivity of LC+HERA*p* based γp collider to anomalous couplings at 95% C.L. for real photons. Only one of the couplings is assumed to deviate from the SM at a time.

$\sqrt{s_{ep}}$(GeV)	$\int L dt$(pb^{-1})	δ^{sys}	$\Delta\kappa$	λ
1715.8	500	0	-0.019, 0.019	-0.048, 0.048
1715.8	500	0.05	-0.040, 0.038	-0.049, 0.049
1356.5	500	0	-0.022, 0.021	-0.053, 0.053
1356.5	500	0.05	-0.042, 0.040	-0.054, 0.054
1356.5	200	0	-0.034, 0.033	-0.067, 0.067
1356.5	200	0.05	-0.050, 0.048	-0.068, 0.068

$$X_i=\int_{V_i}^{V_{i+1}}\frac{d\sigma^{\text{SM}}}{dV}dV, \quad Y_i=\int_{V_i}^{V_{i+1}}\frac{d\sigma^{\text{new}}}{dV}dV, \tag{19}$$

$$\Delta_i^{\text{exp}}=X_i\sqrt{\delta_{\text{stat}}^2+\delta_{\text{sys}}^2}, \quad V=p_T. \tag{20}$$

We have divided p_T region of the final quark into equal pieces for binning procedure and have considered at least 10 events in each bin. For sensitivity, the number of W^+ and W^- events given with their branching ratios in the $\mu\nu$ and $e\nu$ channels has been taken into account. Using the above formula the limits on the $\Delta\kappa$ and λ are given in Table IV for the deviation of the cross section from the standard model value at 95% confidence level with and without systematic error. On the ground of comparison we give the limits from ep collider in Table V using the Weizsäcker-Williams approximation.

From these tables we see that γp mode of LC+HERA*p* probes $\Delta\kappa$ and λ with better sensitivity than Tevatron and individual LEP2 experiments. Combination of the results of the four LEP2 experiments produces sensitivity intervals (difference between the upper and lower limits) $O(10^{-1})$ for $\Delta\kappa$ and λ (see introduction) while LC+HERA*p* gives the same intervals as $O(10^{-2})$ and $O(10^{-1})$, respectively. In the case of sensitivity to $\Delta\kappa$, γp collider is comparable to LHC which can probe $WW\gamma$ and WWZ couplings separately with $W\gamma$ and WZ production. It is anticipated that the future linear e^+e^- colliders can reach the sensitivity of $O(10^{-3})-O(10^{-4})$ depending on the energy and luminosity with mixed couplings of $WW\gamma$ and WWZ vertices for unpolarized beams. The highly polarizable beams at LC allow one to discriminate couplings at the same order of sensitivity as above [22] that have correlated effects on observables with

TABLE V. Sensitivity of LC+HERAp collider to anomalous couplings at 95% C.L. for *WWA*.

$\sqrt{s_{ep}}$(GeV)	$\int L dt$(pb^{-1})	δ^{sys}	$\Delta\kappa$	λ
1715.8	500	0	-0.064, 0.061	-0.124, 0.124
1715.8	500	0.05	-0.079, 0.075	-0.125, 0.125
1356.5	500	0	-0.078, 0.074	-0.175, 0.175
1356.5	500	0.05	-0.090, 0.085	-0.176, 0.176
1356.5	200	0	-0.121, 0.116	-0.250, 0.250
1356.5	200	0.05	-0.135, 0.122	-0.250, 0.250

unpolarized beams. With presently expected luminosities LC+HERAp seems not to be able to attain LC precision. In γe and $\gamma\gamma$ collisions [23] with laser backscattering at basic linear colliders one can probe the $WW\gamma$ couplings with $O(10^{-2})$ precision which are the same order of magnitude as in the γp collision. Reduction in luminosity is expected in In γe and $\gamma\gamma$ collisions when compared to basic e^+e^- collision due to scattering of laser photons. However, almost the same luminosity can be obtained in γp collision as the basic ep collision because of the larger transverse size of the proton beam (see the introduction). As the γe and $\gamma\gamma$ colliders, the γp collider has the advantage of probing $WW\gamma$ couplings independently of WWZ effects. After further improvement of luminosity, linac-ring-type γp collider possibly will give complementary information to LHC and LC.

ACKNOWLEDGMENTS

The authors are grateful to the members of the AUHEP group and S. Sultansoy for drawing our attention to anomalous couplings.

[1] D0 Collaboration, B. Abbott *et al.*, Phys. Rev. D **60**, 072002 (1999).
[2] ALEPH Collaboration, R. Barate *et al.*, Phys. Lett. B **422**, 369 (1998); The DELPHI Collaboration, P. Abreu *et al.*, *ibid.* **423**, 194 (1998); The L3 Collaboration, M. Acciari *et al.*, *ibid.* **467**, 171 (1999); The OPAL Collaboration, G. Abbiendi *et al.*, Eur. Phys. J. C **9**, 191 (1999).
[3] The LEP Collaborations ALEPH, DELPHI, L3, OPAL, and The LEP TGC Working Group, G. Bella *et al.*, Report No. LEPEWWG/TGC/2000-01.
[4] M.N. Dubinin and H.S. Song, Phys. Rev. D **57**, 2927 (1998).
[5] U. Baur, J. Vermaseren, and D. Zeppenfeld, Nucl. Phys. **B375**, 3 (1992).
[6] C.S. Kim, Jungil Lee, and H.G. Song, Z. Phys. C **63**, 673 (1994).
[7] U. Baur and D. Zeppenfeld, Nucl. Phys. **B325**, 253 (1989).
[8] M. Janssen, Z. Phys. C **52**, 165 (1991); M. Böhm and A. Rosado, *ibid.* **39**, 275 (1988).
[9] V.A. Noyes, Proceedings of the Workshop on Future Physics at HERA 1995/96, edited by Ingelman, A. De Roeck, and R. Klanner, p. 190; S. Godfrey, Z. Phys. C **55**, 619 (1992); T. Helbig and H. Spiesberger, Nucl. Phys. **B373**, 73 (1992); U. Baur and M.A. Doncheski, Phys. Rev. D **46**, 1959 (1992).
[10] ATLAS Technical Design Report, Vol. II, 1999.
[11] Conceptual Design Report of LC500, DESY 1997-048.
[12] D. Trines, *Proceedings of the International Workshop on the Linac-Ring Type ep and γp Colliders*, [Turk. J. Phys. **22**, 529 (1998)].
[13] R. Brinkmann, Turk. J. Phys. **22**, 661 (1998); Z.Z. Aydin, A.K. Ciftci, and S. Sultansoy, Nucl. Instrum. Methods Phys. Res. A **351**, 261 (1994).
[14] A. De Roeck, Turk. J. Phys. **22**, 595 (1998).
[15] S.I. Alekhin *et al.*, Int. J. Mod. Phys. A **6**, 21 (1991); A.K. Ciftci, S. Sultansoy, S. Turkoz, and O. Yavas, Nucl. Instrum. Methods Phys. Res. A **365**, 317 (1995); A.K. Ciftci, Turk. J. Phys. **22**, 675 (1998).
[16] Z.Z. Aydin *et al.*, Int. J. Mod. Phys. A **11**, 2019 (1996).
[17] S. Atag and O. Cakir, Phys. Rev. D **49**, 5769 (1994); O. Cakir and S. Atag, J. Phys. G **21**, 1189 (1995); S. Atag, A. Celikel, and S. Sultansoy, Phys. Lett. B **326**, 185 (1994); A.T. Alan, Z.Z. Aydin, and S. Sultansoy, *ibid.* **327**, 70 (1994); A.T. Alan, S. Atag, and Z.Z. Aydin, J. Phys. G **20**, 1399 (1994); A. Kandemir and U. Yilmazer, Phys. Lett. B **385**, 143 (1996).
[18] K.J.F. Gaemers and G.J. Gournaris, Z. Phys. C **1**, 259 (1979).
[19] K. Hagiwara, R.D. Peccei, D. Zeppenfeld, and K. Hikasa, Nucl. Phys. **B282**, 253 (1987).
[20] A.D. Martin, W.J. Stirling, and R.G. Roberts, Phys. Rev. D **51**, 4756 (1995).
[21] M. Drees and K. Grassie, Z. Phys. C **28**, 451 (1985).
[22] V.V. Andreev, A.A. Pankov, and N. Paver, Phys. Rev. D **53**, 2390 (1996); A.A. Likhoded, T. Han, and G. Valencia, *ibid.* **53**, 4811 (1996).
[23] S.Y. Choi and F. Schrempp, Phys. Lett. B **272**, 149 (1991).